

# Convergence of the Discrete Minimum Energy Path\*

Xuanyu Liu<sup>†</sup> Huajie Chen<sup>‡</sup> and Christoph Ortner<sup>§</sup>

## Abstract

The minimum energy path (MEP) describes the mechanism of reaction, and the energy barrier along the path can be used to calculate the reaction rate in thermal systems. The nudged elastic band (NEB) method is one of the most commonly used schemes to compute MEPs numerically. It approximates an MEP by a discrete set of configuration images, where the discretization size determines both computational cost and accuracy of the simulations. In this paper, we consider a discrete MEP to be a stationary state of the NEB method and prove an optimal convergence rate of the discrete MEP with respect to the number of images. Numerical simulations for the transitions of some several proto-typical model systems are performed to support the theory.

## 1 Introduction

In computational chemistry, the reaction mechanism is often represented by a reaction path on the potential energy landscape, which is of great importance to determine the thermodynamic and kinetic properties of chemical reactions. The minimum energy path (MEP) has been most widely used to represent the reaction path, giving the route that needs the least amount of work for the system to undergo the transition. The MEP connects two local minimizers and goes through one or more transition state (saddle), along which the energy barrier (at the saddle) can be used to calculate the transition rate (see e.g. [1, 6, 16]) of the reaction.

The most widely used techniques for finding the MEP are the nudged elastic band (NEB) method [7, 8] and the string method [4, 5, 15]. They both iteratively evolve a discrete path of images in projected steepest descent directions, while keeping a smooth distribution of the images along the path. The number of images along the path determines the accuracy and efficiency of the simulation, especially when the energy functional is expensive to evaluate (for example, when the system is described by quantum mechanical models). This makes it particularly important to obtain sharp error bounds of the MEP approximation with respect to the number of images.

---

\*This work was supported by the National Key R&D Program of China (No. 2020YFA0712900). HC's work was also supported by National Natural Science Foundation of China (No. NSFC11971066).

<sup>†</sup>xyliu9535@mail.bnu.edu.cn. School of Mathematical Sciences, Beijing Normal University, Beijing 100875, China.

<sup>‡</sup>chen.huajie@bnu.edu.cn. School of Mathematical Sciences, Beijing Normal University, Beijing 100875, China.

<sup>§</sup>ortner@math.ubc.ca. Department of Mathematics, University of British Columbia, 1984 Mathematics Road, Vancouver, BC, Canada V6T 1Z2.

Notwithstanding the importance of such a convergence analysis, there is in general very limited work devoted to the analysis of the MEP. In [3], the authors give a comprehensive qualitative analysis of the evolution of the path by the string method from a dynamical systems perspective, characterizing the set of limiting curves and establishing conditions under which the limiting curve is indeed a MEP. The techniques of this work are not suitable to perform a numerical discretization analysis.

In [9], the authors investigated and analyzed the convergence of the string method. Under some assumptions related to the critical points, they proposed a uniform asymptotic stability of the MEP in the sense that any curve near the MEP can be arbitrarily close to it in the Hausdorff distance under the gradient decent dynamics. With this stability concept they showed that the string method initialized in a neighborhood of the MEP can converge to an arbitrarily small neighborhood of the limiting MEP as the number of images is increased. However, for a curve near the MEP, this notion of stability does not give an explicit relationship between its deviation to the MEP and its force, hence it may not be able to provide an *error bound* with respect to the number of images.

To prepare for a comprehensive and sharp convergence analysis of the NEB and string methods, we began in [11] to establish a new framework for studying the stability of MEPs. We showed that the displacement of a curve to the MEP can be directly bounded by its force under appropriate weighted function space norms. This result in particular directly implies the stability of MEPs under perturbations of the potential energy landscape. Our result also suggests a path towards studying the convergence of the discrete MEP, to which end we still need an analogous stability for the discrete MEP (see Section 4.2).

The purpose of the present work is to obtain such a discrete stability result and hence deduce sharp convergence rates of discrete MEPs to their continuous limits. Under mild and natural assumptions on the limit MEP, we will indeed obtain an optimal convergence rate. More precisely, we will show that (see Theorem 2.1)

$$\|\bar{\varphi} - \bar{\varphi}_M\| \leq CM^{-1},$$

where  $\bar{\varphi}$  and  $\bar{\varphi}_M$  are the MEP and the discrete MEP respectively,  $\|\cdot\|$  denotes a discrete  $C^1$ -type-norm while  $M$  is the number of images used to discretize the path. To our best knowledge, this is the first result that gives an explicit convergence rate for the MEP with respect to the discretization parameters.

**Outline.** The rest of this paper is organized as follows. In Section 2, we present the main results of this paper, including the convergence result and numerical experiments. In Section 3, we give some conclusions. In Section 4, we present detailed proofs for the convergence results.

**Notation.** Denote the Euclidean norm and  $\ell^\infty$ -norm of a vector by  $|\cdot|$  and  $|\cdot|_\infty$ , respectively. And  $\|\cdot\|_\infty$  is used to denote the matrix norm induced by  $|\cdot|_\infty$ . For  $b > a$ , we denote by  $C([a, b]; \mathbb{R}^N)$  the space of continuous curves in the configuration space  $\mathbb{R}^N$  with the norm  $\|\varphi\|_{C([a, b]; \mathbb{R}^N)} := \sup_{\alpha \in [a, b]} |\varphi(\alpha)|_\infty$ ; and  $C^1([a, b]; \mathbb{R}^N)$  the space of continuously differentiable curves with the norm  $\|\varphi\|_{C^1([a, b]; \mathbb{R}^N)} := \|\varphi\|_{C([a, b]; \mathbb{R}^N)} + \|\varphi'\|_{C([a, b]; \mathbb{R}^N)}$ . Let  $X$  and  $Y$  be Banach spaces with the norm  $\|\cdot\|_X$  and  $\|\cdot\|_Y$  respectively. We will denote by  $\mathcal{L}(X, Y)$  the Banach space of all linear bounded operators from  $X$  to  $Y$  with the operator norm  $\|\cdot\|_{\mathcal{L}(X, Y)}$ . For a given functional  $\mathcal{F} \in C^1(X)$ , we will denote its first variation by  $\delta\mathcal{F}(x)v$  with  $v \in X$ . We will use  $C$  to denote a generic positive constant that may change from one line to the next. In the error estimates,  $C$  will always be independent on the discretization parameters or the choice of test functions. The dependencies of  $C$  on model parameters (in our context, the energy landscape) will normally be clear from the context or stated explicitly.

## 2 Main results

### 2.1 Minimum energy path

Let  $E : \mathbb{R}^N \rightarrow \mathbb{R}$  be a potential energy functional with  $N \in \mathbb{N}$  the dimensionality of the configuration space, which could encode atomic positions, the structure of crystal lattices, a discretization of a function space, and many other examples. Throughout this paper we assume that  $E \in C^4(\mathbb{R}^N)$ . This regularity assumption is required because we will need to control perturbations of the eigenvalues and eigenvectors of the Hessian  $\nabla^2 E$  to be  $C^2$  in our analysis.

Given an energy function  $E$ , we call  $y \in \mathbb{R}^N$  a critical point if  $\nabla E(y) = 0$ . We call a critical point  $y$  a strong local minimizer if the Hessian  $\nabla^2 E(y) \in \mathbb{R}^{N \times N}$  is positive definite, and an index-1 saddle point if  $\nabla^2 E(y)$  has exactly one negative eigenvalue while all the other eigenvalues are positive. For the sake of brevity we will omit the qualifiers “strong” and “index-1” and simply say “local minimizer” and “saddle point”. We assume throughout that  $E$  has at least two local minimizers on the energy landscape denoted, respectively, by  $y_M^A \in \mathbb{R}^N$  and  $y_M^B \in \mathbb{R}^N$ .

A minimum energy path (MEP) is a curve  $\varphi \in C^1([0, 1]; \mathbb{R}^N)$  connecting  $y_M^A$  and  $y_M^B$  whose tangent is everywhere parallel to the gradient except at the critical points. To give a rigorous definition of the MEP, we first define two projection operators  $P_v, P_v^\perp : \mathbb{R}^N \rightarrow \mathbb{R}^N$  with a given a vector  $v \in \mathbb{R}^N \setminus \{0\}$ , by  $P_v := vv^T / |v|^2$  and  $P_v^\perp := I - P_v$ , where  $I \in \mathbb{R}^{N \times N}$  is the identity matrix. Define the admissible class for “regular” curves connecting the minimizers  $y_M^A$  and  $y_M^B$  as

$$\mathcal{A} := \left\{ \varphi \in C^1([0, 1]; \mathbb{R}^N) : \varphi(0) = y_M^A, \varphi(1) = y_M^B, \varphi'(\alpha) \neq 0 \quad \forall \alpha \in [0, 1] \right\}.$$

Then a MEP connecting the minimizers  $y_M^A$  and  $y_M^B$  is a solution of the following problem: Find  $\varphi \in \mathcal{A}$  such that

$$\begin{cases} P_{\varphi'(\alpha)}^\perp \nabla E(\varphi(\alpha)) = 0 & \forall \alpha \in [0, 1], \\ |\varphi'(\alpha)| - L(\varphi) = 0 & \forall \alpha \in [0, 1], \end{cases} \quad (2.1a)$$

$$(2.1b)$$

where  $L : C^1([0, 1]; \mathbb{R}^N) \rightarrow \mathbb{R}$  is the length operator given by  $L(\varphi) := \int_0^1 |\varphi'(s)| \, ds$ . Equation (2.1b) enforces the curve to be parameterized by normalized arc length, which removes the redundancy due to re-parameterization. With this additional constraint one intuitively expects that the MEP is locally unique, at least under some further natural assumptions that we now formalize:

If  $\bar{\varphi}$  is a solution of (2.1), since  $y_M^A$  and  $y_M^B$  are local minimizers, there exists an  $\bar{s} \in (0, 1)$  with  $y_S = \bar{\varphi}(\bar{s}) \in \mathbb{R}^N$  such that the energy  $E(y_S)$  reaches the maximum along the MEP. This implies that  $\nabla E(y_S)$  vanishes in the tangent direction  $\bar{\varphi}'(\bar{s})$  and thus it is a critical point. Since the energy  $E(y_S)$  is a maximum along the tangent  $\bar{\varphi}'(\bar{s})$ , we may generically expect that the Hessian  $\nabla^2 E(y_S)$  has at least one negative eigenvalue. For the sake of simplicity of the analysis, we will assume throughout this paper that

**(A)**  $y_S$  is the *only* critical point between  $y_M^A$  and  $y_M^B$  along the MEP  $\bar{\varphi}$ . Moreover,  $y_M^A, y_M^B$  are strong minimizers, while  $y_S = \bar{\varphi}(\bar{s})$  is an *index-1 saddle*.

Although **(A)** is natural and will be satisfied by *many* (if not most) MEPs one encounters in practice, there are also cases where this assumption fails. For example, in [10] examples

are given where there is more than one *index-1 saddle* along an MEP. Our theory can be generalized to these cases by adjusting the formulations, provided that all critical points along the MEP satisfy certain stability conditions.

We observe by a direct calculation (see Lemma 4.1 for details) that, if  $\bar{\varphi} \in C^2([0, 1]; \mathbb{R}^N)$  solves (2.1), then  $\bar{\varphi}'(0)$ ,  $\bar{\varphi}'(\bar{s})$  and  $\bar{\varphi}'(1)$  are eigenvectors of the Hessians  $\nabla^2 E(y_M^A)$ ,  $\nabla^2 E(y_S)$  and  $\nabla^2 E(y_M^B)$ , respectively. This implies that the MEP has to go through the critical points in the direction of some eigenvector of the corresponding Hessian. The following assumption formalizes the requirement that, to highest order, there is a unique optimal path to exit the energy minimizer.

**(B)** Let  $\sigma_A$  and  $\sigma_B$  denote the eigenvalues associated, respectively, with the eigenvectors  $\bar{\varphi}'(0)$ ,  $\bar{\varphi}'(1)$ . We assume (i) that they are the lowest eigenvalues of  $\nabla^2 E(y_M^A)$  and  $\nabla^2 E(y_M^B)$ ; and (ii) that they are simple.

## 2.2 The discrete MEP and its convergence

We now describe the discretization of the MEP. A natural way to approximate the continuous MEP curve is to use a discrete path of images connecting the two minimizers. The images can best be thought of as interpolated by a spline. The most widely used methods using this idea are the nudged elastic band (NEB) method and the string method. In this paper, we will employ the NEB formulation to define the discrete MEP, but our results can also be applied to the string method provided that the same finite difference scheme as in the NEB method is used to approximate the tangent (see Remark 2.2).

Let  $M \in \mathbb{Z}_+$  be the number of images and  $h := \frac{1}{M}$  be the corresponding meshsize. Let

$$\mathcal{A}_h := \left\{ \phi_h := \{\phi_{h,k}\}_{k=0}^M \in (\mathbb{R}^N)^{M+1} : \phi_{h,0} = y_M^A, \phi_{h,M} = y_M^B, \text{ and } \phi_{h,j} \neq \phi_{h,k} \forall j \neq k \right\}$$

be the space for the discrete path connecting the two minimizers  $y_M^A$  and  $y_M^B$  with  $M + 1$  images.

Given an initial discrete path  $\phi_h^0 \in \mathcal{A}_h$ , the NEB evolution equation is to find a  $\phi_h \in C^1([0, +\infty); \mathcal{A}_h)$  such that

$$\begin{cases} \dot{\phi}_h(t) = \mathcal{F}(\phi_h(t)) & \forall t > 0, \\ \phi_h(0) = \phi_h^0. \end{cases} \quad (2.2)$$

Here the driving force  $\mathcal{F} : \mathcal{A}_h \rightarrow (\mathbb{R}^N)^{M+1}$  is defined by

$$(\mathcal{F}(\phi_h))_k := \begin{cases} 0 & \text{for } k = 0, M, \\ -P_{\hat{\tau}_k}^\perp \nabla E(\phi_{h,k}) + ch^{-1} \left( |\phi_{h,k} - \phi_{h,k+1}| - |\phi_{h,k} - \phi_{h,k-1}| \right) \hat{\tau}_k & \\ 0 & \text{for } k = 1, \dots, M-1, \end{cases} \quad (2.3)$$

where  $c$  is a parameter specifying the balance between the tangential force and the projected downward pull from the curvature of the potential barrier [8], and  $\hat{\tau}_k$  is the normalized tangent

direction at  $\phi_{h,k}$  defined through an upwind scheme

$$\hat{\tau}_k := \frac{(D_h \phi_h)_k}{|(D_h \phi_h)_k|} \quad \text{with}$$

$$(D_h \phi_h)_k := \begin{cases} \frac{\phi_{h,k+1} - \phi_{h,k}}{h} & \text{if } k = 0 \text{ or } E(\phi_{h,k+1}) > E(\phi_{h,k}) > E(\phi_{h,k-1}), \\ \frac{\phi_{h,k} - \phi_{h,k-1}}{h} & \text{if } k = M \text{ or } E(\phi_{h,k-1}) > E(\phi_{h,k}) > E(\phi_{h,k+1}), \\ \frac{\phi_{h,k+1} - \phi_{h,k-1}}{2h} & \text{otherwise.} \end{cases} \quad (2.4)$$

In (2.3), the force perpendicular to the tangent  $\hat{\tau}_k$  is to push the path towards the MEP, while the force parallel to the tangent  $\hat{\tau}_k$  is to enforce an approximate equidistribution of the images along the path.

It is intuitive to expect that the NEB evolution path converges to the MEP in the limit as  $t \rightarrow \infty$  and  $M \rightarrow \infty$ . In the present paper, we focus on the discretization error of the curve, i.e. the limit  $M \rightarrow \infty$ , while the convergence of the evolution, i.e., the limit  $t \rightarrow \infty$ , will be considered in our future work. Let  $\bar{\phi}_h \in \mathcal{A}_h$  be a stationary solution of the NEB evolution equation (2.2). Then  $\bar{\phi}_h$  solves the equation

$$\mathcal{F}(\bar{\phi}_h) = 0, \quad (2.5)$$

and we will call it a discrete MEP.

The following theorem is the main result of this paper, which states the convergence and convergence rate of the discrete MEP to the continuous one. The proof of this theorem is given in Section 4. We not only consider the convergence of the path (under some discrete  $C^1$ -norm), but also the convergence of the approximate energy barrier. For a given path  $\varphi \in \mathcal{A}$ , its energy barrier can be written as

$$\delta E(\varphi) := \sup_{\alpha \in [0,1]} E(\varphi(\alpha)) - E(\varphi(0)).$$

Note that for a MEP  $\bar{\varphi}$ , the energy barrier is completely determined by the energy at the saddle. Correspondingly, we can define the energy barrier of a discrete path  $\phi_h \in \mathcal{A}_h$  by

$$\delta E(\phi_h) := \max_{0 \leq k \leq M} E(\phi_{h,k}) - E(\phi_{h,0}),$$

with a bit of abuse of the notation  $\delta E$ .

**Theorem 2.1.** *Let  $\bar{\varphi} \in C^3([0, 1]; \mathbb{R}^N)$  be a solution of (2.1). Assume that **(A)** and **(B)** are satisfied. Then for sufficiently small  $h$ , there exists a solution  $\bar{\phi}_h$  of (2.5) such that*

$$\max_{0 \leq k \leq M} |(D_h \bar{\phi}_h)_k - \bar{\varphi}'(kh)| + \max_{0 \leq k \leq M} |\bar{\phi}_{h,k} - \bar{\varphi}(kh)| \leq C_p h \quad \text{and} \quad (2.6)$$

$$|\delta E(\bar{\varphi}) - \delta E(\bar{\phi}_h)| \leq C_e h^2, \quad (2.7)$$

where  $C_p$  and  $C_e$  are positive constants depending only on  $E$  and  $\bar{\varphi}$ ,

**Remark 2.1.** *In our convergence analysis, we only consider numerical schemes that approximate the tangent by first order finite differences (see the definition of the upwind scheme in (2.4)). Therefore, the  $\mathcal{O}(h)$  convergence rate in Theorem 2.1 is optimal. Since the MEP itself*

is typically used only to extract qualitative information this is sufficient for most applications. The quantitative accuracy of the energy barrier is more important for the accurate prediction of transition rates. If the accuracy provided by the MEP is insufficient then one can easily improve on the prediction, e.g. using a dimer method or a Krylov-Newton method, taking the maximum along the MEP as the initial guess.

**Remark 2.2.** Theorem 2.1 gives the convergence of the discrete MEP obtained by the NEB method. For the other widely used method, the string method, the discrete path  $\phi_h$  is evolved by the driving force

$$(\mathcal{F}^{\text{string}}(\phi_h))_k := -P_{(D_h\phi_h)_k}^\perp \nabla E(\phi_{h,k}) \quad \text{for } k = 1, \dots, M-1.$$

Instead of using a force in tangent direction as that in the NEB method, a redistribution of the images is performed at each step during the evolution [5]. Then the discrete MEP defined by the stationary state of the string method  $\bar{\phi}_h^{\text{string}}$  is such that the force  $\mathcal{F}^{\text{string}}$  vanishes and the images are equally distributed along the path. This implies  $\mathcal{F}(\bar{\phi}_h^{\text{string}}) = 0$ , and thus  $\bar{\phi}_h^{\text{string}}$  is exactly the same path as that obtained by the NEB method. Therefore, the convergence result also holds for the discrete MEP from the string method.

However, many implementations of the string method employ cubic spline interpolation to obtain the tangent and additional work would be required to extend our analysis to those schemes.

## 2.3 Numerical experiments

We carry out some numerical experiments for the transitions of some typical systems, to support and extend the theoretical results. All simulations are implemented in open-source Julia packages JuLIP.jl [14], and performed on a PC with Intel Core i7-CPU (2.2 GHz) with 32GB RAM. To test the decay of the numerical errors, the results obtained by a very fine discretization (with up to 1000 images) are used as the reference MEP.

To support the theory developed in this paper, we test the convergence in the discrete  $C^1$ -norm error (see (2.6)) and of the energy barrier error (see (2.7)) of the discrete MEP. For completeness, we also test the convergence in a discrete max-norm. These three error measures are, respectively, denoted by

$$\begin{aligned} e_{h,C^1} &:= \max_{0 \leq k \leq M} |(D_h \bar{\phi}_h)_k - \bar{\varphi}'(kh)| + \max_{0 \leq k \leq M} |\bar{\phi}_{h,k} - \bar{\varphi}(kh)|, \\ e_{h,E_b} &:= |\delta E(\bar{\varphi}) - \delta E(\bar{\phi}_h)| \quad \text{and} \\ e_{h,C} &:= \max_{0 \leq k \leq M} |\bar{\phi}_{h,k} - \bar{\varphi}(kh)|. \end{aligned}$$

**Example 1.** Consider a toy model with the potential  $E : \mathbb{R} \times \mathbb{R}_+ \rightarrow \mathbb{R}$  with

$$E(x, y) = (1 - x^2 - y^2)^2 + \frac{y^2}{x^2 + y^2} \quad y \geq 0.$$

The contour lines of the energy landscape are shown in Figure 2.1. We see that there are two minimizers located at  $(-1, 0)$  and  $(1, 0)$ , respectively. We present the decay of the numerical errors in Figure 2.2. We observe that the convergence rate of the discrete  $C^1$ -norm error is  $\mathcal{O}(h)$  and that of the energy barrier error is  $\mathcal{O}(h^2)$ , which agrees with our theory. We further

observe that the discrete  $C$ -norm error decays with the same rate as the discrete  $C^1$ -norm error, i.e., there is no improved rate when employing a weaker norm. This suggests that the spaces we employed in the analysis are in fact natural.

In the above energy functional, the eigenvalues of  $\nabla^2 E(y_M^A)$  are 2 and 8, and  $\sigma_A = 2$  is simple and the lowest eigenvalue. As comparisons, we test two other energy functionals with similar form but not satisfying the condition **(B)**. First, let  $E_1 : \mathbb{R} \times \mathbb{R}_+ \rightarrow \mathbb{R}$  be given by

$$E_1(x, y) = \frac{1}{4}(1 - x^2 - y^2)^2 + \frac{y^2}{x^2 + y^2} \quad y \geq 0.$$

The Hessian  $\nabla^2 E_1(y_M^A)$  has an eigenvalue 2 with multiplicity 2, so  $\sigma_A = 2$  is the lowest but a degenerated eigenvalue of  $\nabla^2 E_1(y_M^A)$ . Note that the exact MEP of this case is explicitly known as the upper and lower branches of the unit circle, from which we can calculate the exact numerical errors. We present the contour lines of the energy landscape and the decay of numerical errors in Figure 2.3 and 2.4 respectively. Secondly, let  $E_2 : \mathbb{R} \times \mathbb{R}_+ \rightarrow \mathbb{R}$  be given by

$$E_2(x, y) = \frac{1}{8}(1 - x^2 - y^2)^2 + \frac{y^2}{x^2 + y^2} \quad y \geq 0.$$

The eigenvalues of  $\nabla^2 E_2(y_M^A)$  are 2 and 1, in which  $\sigma_A = 2$  is simple but not the lowest eigenvalue. The exact MEP of this case is also known as the upper and lower branches of the unit circle. We show the contour lines of the energy landscape and the decay of numerical errors in Figure 2.5 and 2.6 respectively. In the last two examples, we see that the discrete MEP also converge in discrete  $C^1$ -norm, but the convergence rates are significantly slower and it is only  $O(h^{1/2})$  for the last case. This indicates that the condition **(B)** is really necessary to obtain Theorem 2.1. But surprisingly, we find that the discrete  $C$ -norm error and the energy barrier error still decay as  $O(h)$  and  $O(h^2)$ , respectively. The methods of our present work are insufficient to explain these effects; obtaining sharp rates in the linearly unstable regime will require further work.

**Example 2.** Next, we consider the Muller potential [12]  $E : \mathbb{R} \times \mathbb{R} \rightarrow \mathbb{R}$  with

$$E(x, y) = \sum_{k=1}^4 T_k \exp \left( a_k(x - \bar{x}_k)^2 + b_k(x - \bar{x}_k)(y - \bar{y}_k) + c_k(y - \bar{y}_k)^2 \right),$$

where the parameters are  $T = (-200, -100, -170, -15)^T$ ,  $a = (-1, -1, -6.5, 0.7)^T$ ,  $b = (0, 0, 11, 0.6)^T$ ,  $c = (-10, -10, -6.5, 0.7)^T$ ,  $\bar{x} = (1, 0, -0.5, -1)^T$  and  $\bar{y} = (0, 0.5, 1.5, 1)^T$ . We present the contour lines of energy landscape in Figure 2.7 and the decay of numerical errors in Figure 2.8. We again observe an  $\mathcal{O}(h)$  decay for the discrete  $C^1$ -norm and  $C$ -norm errors, and  $\mathcal{O}(h^2)$  for the energy barrier error.

**Example 3.** Consider a two dimensional periodic system with two atoms lying in each unit cell. In the “first” cell containing the origin, we fix one atom at the origin and put the other at the position  $(x, y) \in \mathbb{R}^2$ , and then construct a corresponding lattice  $\Lambda := \begin{pmatrix} 2x & x \\ 0 & y \end{pmatrix} \mathbb{Z}^2$  (see Figure 2.9). The interaction between any two atoms in the lattice  $\Lambda$  is modelled by the Lennard-Jones pair potential

$$\phi(r) = 4\epsilon_0 \left( \left( \frac{\sigma_0}{r} \right)^{12} - \left( \frac{\sigma_0}{r} \right)^6 \right) \phi_{\text{cut}}(r)$$

with parameters  $\epsilon_0 = 1$ ,  $\sigma_0 = 1$  and a cubic spline cut-off function [2]  $\phi_{\text{cut}}$  satisfying  $\phi_{\text{cut}}(r) = 1$  for  $r \in [0, 1.9]$  and  $\phi_{\text{cut}}(r) = 0$  for  $r \geq 2.7$ . Then the “averaged” energy of the system (i.e.

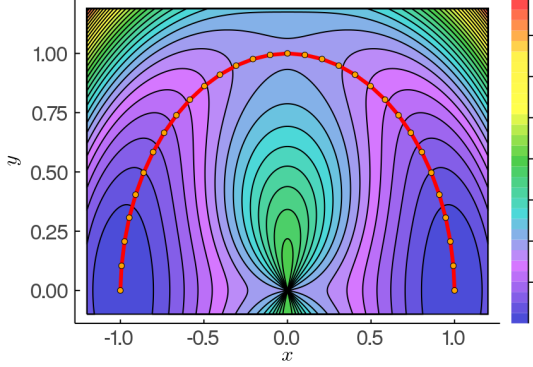


Figure 2.1: (Example 1) The contour lines of the energy landscape for  $E$ , with two minimizers and the MEP (red line).

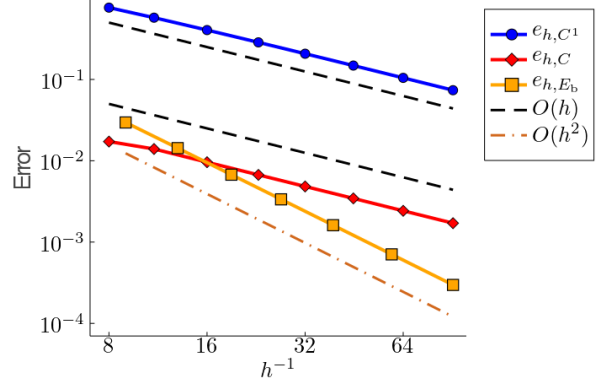


Figure 2.2: (Example 1) The convergence of the discrete MEP ( $\sigma_A$  is simple and lowest eigenvalue).

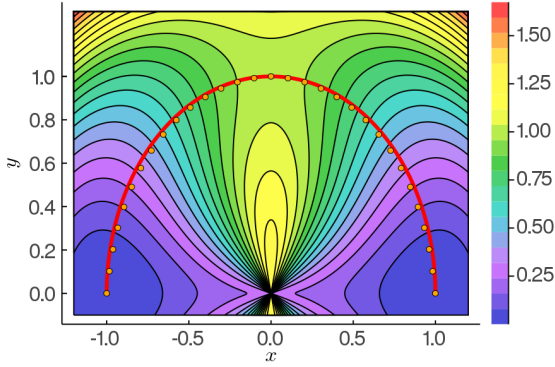


Figure 2.3: (Example 1) The contour lines of the energy landscape for  $E_1$ , with two minimizers and the MEP (red line).

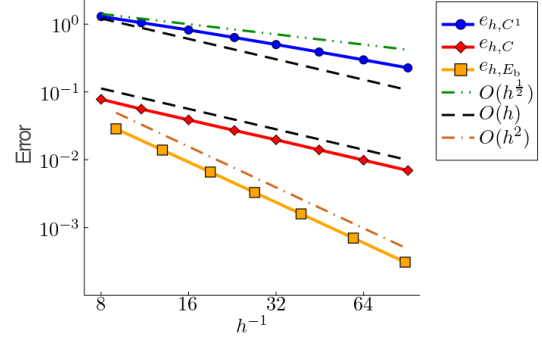


Figure 2.4: (Example 1) The convergence of the discrete MEP ( $\sigma_A$  is a degenerated eigenvalue).

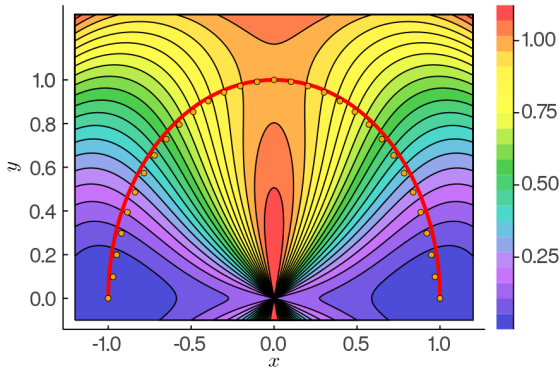


Figure 2.5: (Example 1) The contour lines of the energy landscape for  $E_2$ , with two minimizers and the MEP (red line).

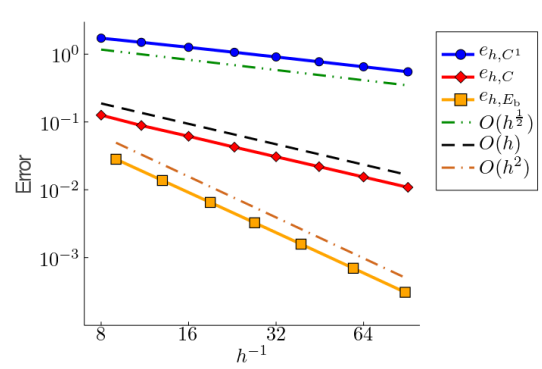


Figure 2.6: (Example 1) The convergence of the discrete MEP ( $\sigma_A$  is not the lowest eigenvalue).

energy per cell) is the sum of the site energy of the two atoms located at origin and  $(x, y)$ ,

$$E(x, y) = \frac{1}{2} \sum_{(x', y') \in \Lambda} \phi(|(x', y') - (0, 0)|) + \frac{1}{2} \sum_{(x', y') \in \Lambda} \phi(|(x', y') - (x, y)|).$$



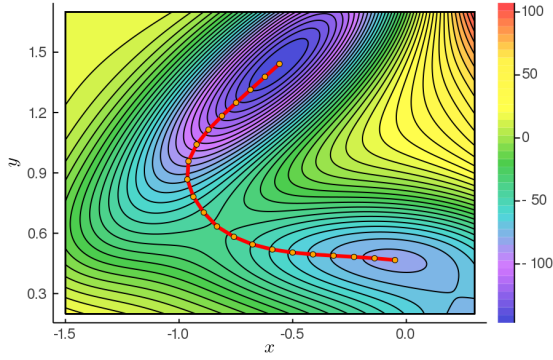


Figure 2.7: (Example 2) The contour lines of the energy landscape, with two minimizers and the MEP (red line).

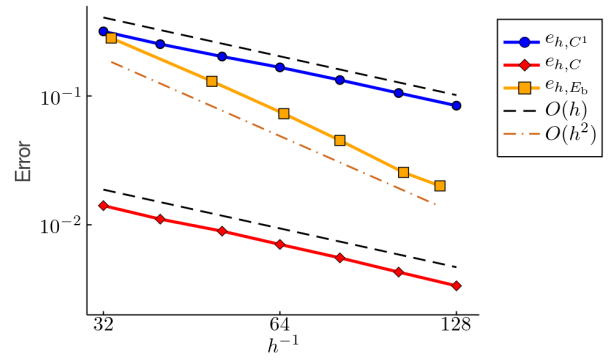


Figure 2.8: (Example 2) Convergence of the discrete MEP.

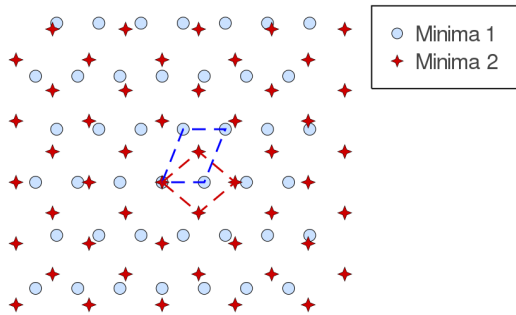


Figure 2.9: (Example 3) The configurations of two minimizers.

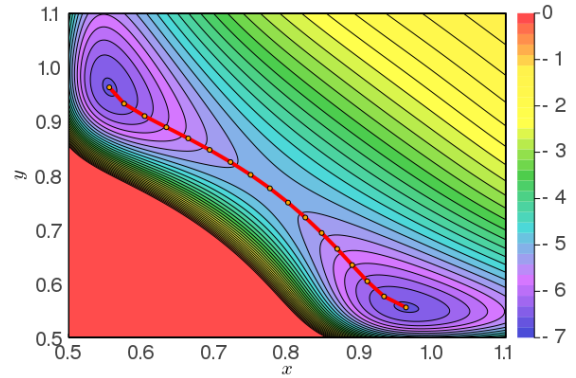


Figure 2.10: (Example 3) The contour lines of energy landscape, with two minimizers and the MEP (red line). Since the energy explodes when the two atoms collide, we only show the contour lines with energy less than 0.

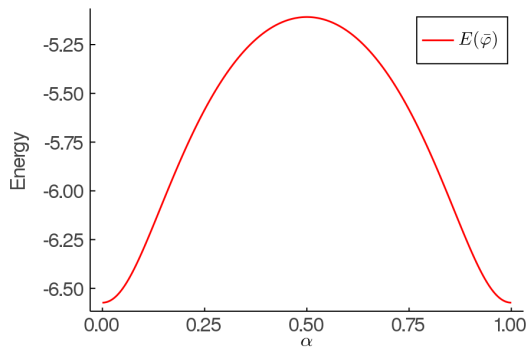


Figure 2.11: (Example 3) Energy path of MEP

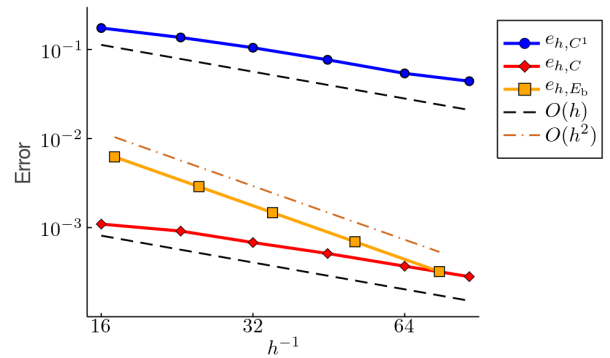


Figure 2.12: (Example 3) Convergence of the discrete MEP.

We present the contour lines of the energy landscape in Figure 2.10, together with the two minimizers and the MEP. We further present the energy path of the MEP in Figure 2.11.

The decay of the numerical errors are shown in Figure 2.12, from which we observe an  $\mathcal{O}(h)$  convergence rate for the discrete  $C^1$ -norm and discrete  $C$ -norm errors, and an  $\mathcal{O}(h^2)$  convergence rate for the energy barrier error.

### 3 Conclusions

This paper studies the convergence of the discrete MEPs that are given by the stationary states of the NEB methods. We establish an optimal convergence rate of the discrete MEP with respect to the number of images along the path. For numerical methods that find the MEP by evolving the path between local minimizers (say NEB methods and string methods), an important remaining issue is the convergence with respect to the evolution time, which will be studied in our other work.

## 4 Proofs: Convergence of the discrete MEP

In this section, we will provide a proof of Theorem 2.1. We will first propose abstract forms for the MEP equation (2.1) and the corresponding discretization; then give a stability result of the discrete MEP; and finally derive the convergence by connecting the abstract discrete MEP equation with (2.5).

### 4.1 The abstract MEP and discrete MEP equations

Define an abstract MEP operator  $\mathcal{F} : \mathcal{A} \rightarrow C([0, 1]; \mathbb{R}^N)$  with

$$\mathcal{F}(\varphi)(\alpha) := P_{\varphi'(\alpha)}^\perp \nabla E(\varphi(\alpha)) - \alpha(\alpha - 1)(\alpha - \bar{s})(|\varphi'(\alpha)| - L(\varphi)) \frac{\varphi'(\alpha)}{|\varphi'(\alpha)|} \quad (4.1)$$

for  $\alpha \in [0, 1]$ . Then we can bring in an abstract form of (2.1): Find  $\varphi \in \mathcal{A}$  such that

$$\mathcal{F}(\varphi) = 0. \quad (4.2)$$

Comparing the components of  $\mathcal{F}$  with (2.1), we see that  $\bar{\varphi}$  solves (2.1) if and only if it is a solution of (4.2).

Consider a discrete path with  $M + 1$  ( $M \in \mathbb{Z}_+$ ) images. Let  $h = \frac{1}{M}$  be the corresponding mesh size. We denote by  $\alpha_k := kh$  ( $k = 0, \dots, M$ ) the nodes of the discrete path. Since  $E(y_S)$  reaches the maximum along the MEP, there exists a  $k_{\bar{s}} \in \mathbb{Z}_+$  such that  $\alpha_{k_{\bar{s}}} \in (\bar{s} - h, \bar{s} + h)$  and  $E(\bar{\varphi}(\alpha_{k_{\bar{s}}})) = \max_{0 \leq k \leq M} E(\bar{\varphi}(\alpha_k))$ . Note that  $\alpha_{k_{\bar{s}}}$  is to approximate the index  $\bar{s}$  and  $\lim_{h \rightarrow 0^+} \alpha_{k_{\bar{s}}} = \bar{s}$ .

To deduce a discretization of (4.2), we first introduce two first order difference operators. Define  $\tilde{D}_h, \hat{D}_h : (\mathbb{R}^N)^{M+1} \rightarrow (\mathbb{R}^N)^{M+1}$  with

$$(\tilde{D}_h \varphi_h)_k := \begin{cases} \frac{\varphi_{h,k+1} - \varphi_{h,k}}{h} & \text{for } k = 0, \dots, k_{\bar{s}} - 1 \\ \frac{\varphi_{h,k+1} - \varphi_{h,k-1}}{2h} & \text{for } k = k_{\bar{s}} \\ \frac{\varphi_{h,k} - \varphi_{h,k-1}}{h} & \text{for } k = k_{\bar{s}} + 1, \dots, M \end{cases} \quad \text{and} \quad (4.3)$$

$$(\hat{D}_h \varphi_h)_k := \begin{cases} \frac{\varphi_{h,k+1} - \varphi_{h,k}}{h} & \text{for } k = 0 \\ \frac{\varphi_{h,k} - \varphi_{h,k-1}}{h} & \text{for } k = 1, \dots, M \end{cases}. \quad (4.4)$$

Let

$$Y_h := \{f_h = \{f_{h,k}\}_{k=0}^M \in (\mathbb{R}^N)^{M+1} : f_{h,0} = f_{h,M} = 0\}$$

equipped with the norm

$$\|f_h\|_{Y_h} := \max_{1 \leq k \leq M-1} \left| \frac{f_{h,k}}{\alpha_k(\alpha_k - 1)} \right|_\infty + \max_{\substack{0 \leq k \leq M, \\ k \neq k_{\bar{s}}}} \left| \frac{f_{h,k} - f_{h,k_{\bar{s}}}}{\alpha_k - \alpha_{k_{\bar{s}}}} \right|_\infty. \quad (4.5)$$

Define  $\mathcal{F}_h : \mathcal{A}_h \rightarrow Y_h$  by

$$(\mathcal{F}_h(\varphi_h))_k := P_{(\hat{D}_h \varphi_h)_k}^\perp \nabla E(\varphi_{h,k}) - \alpha_k(\alpha_k - 1)(\alpha_k - \alpha_{k_{\bar{s}+\frac{1}{2}}}) (|\hat{D}_h \varphi_h|_k - L_h(\varphi_h)) \frac{(\hat{D}_h \varphi_h)_k}{|(\hat{D}_h \varphi_h)_k|} \quad (4.6)$$

for  $k = 0, \dots, M$ , where  $\alpha_{k_{\bar{s}+\frac{1}{2}}} := (k_{\bar{s}} + \frac{1}{2})h$  and  $L_h : \mathcal{A}_h \rightarrow \mathbb{R}$  is a discretization of the length operator  $L$

$$L_h(\varphi_h) := h \sum_{k=1}^M |(\hat{D}_h \varphi_h)_k| = \sum_{k=1}^M |\varphi_{h,k} - \varphi_{h,k-1}|. \quad (4.7)$$

We can then provide a discretization of (4.2): Find  $\varphi_h \in \mathcal{A}_h$  such that

$$\mathcal{F}_h(\varphi_h) = 0. \quad (4.8)$$

Then the solution  $\bar{\varphi}_h$  of (4.8) will be taken as an approximation of MEP  $\bar{\varphi}$ . We observe from (4.4), (4.7) and (4.8) that

$$|\bar{\varphi}_{h,k} - \bar{\varphi}_{h,k-1}| = |\bar{\varphi}_{h,k} - \bar{\varphi}_{h,k+1}| \quad \forall k = 1, \dots, M-1. \quad (4.9)$$

This implies that the images on  $\bar{\varphi}_h$  are equally distributed.

To give the first variation of  $\mathcal{F}$  at  $\bar{\varphi}$ , we introduce a function measuring the gradient of MEP, which will be heavily used in our analysis. Let

$$\bar{\lambda}(\alpha) := \nabla E(\bar{\varphi}(\alpha))^T \frac{\bar{\varphi}'(\alpha)}{|\bar{\varphi}'(\alpha)|^2}, \quad \alpha \in [0, 1]. \quad (4.10)$$

We see from (2.1a) that

$$\nabla E(\bar{\varphi}(\alpha)) = \bar{\lambda}(\alpha) \bar{\varphi}'(\alpha) \quad \text{for } \alpha \in [0, 1], \quad (4.11)$$

The following lemma states the properties of  $\bar{\lambda}$  and it can be seen from [11, Lemma 4.1]. We also observe from the following lemma that  $\sigma_A = \bar{\lambda}'(0)$  and  $\sigma_B = \bar{\lambda}'(1)$ .

**Lemma 4.1.** [11, Lemma 4.1] *Let  $\bar{\varphi} \in C^2([0, 1]; \mathbb{R}^N)$  be the solution of (2.1). If **(A)** is satisfied, then*

(i)  $(\bar{\lambda}'(0), \bar{\varphi}'(0))$ ,  $(\bar{\lambda}'(\bar{s}), \bar{\varphi}'(\bar{s}))$  and  $(\bar{\lambda}'(1), \bar{\varphi}'(1))$  are eigenpairs of the Hessians  $\nabla^2 E(y_M^A)$ ,  $\nabla^2 E(y_S)$  and  $\nabla^2 E(y_M^B)$ , respectively;

(ii)  $\bar{\lambda}'(0) > 0$ ,  $\bar{\lambda}'(1) > 0$  and  $\bar{\lambda}'(\bar{s}) < 0$ ; and

(iii) there exist positive constants  $\underline{c}, \bar{c}$  depending only on  $\bar{\varphi}$ , such that

$$\underline{c} \leq \left| \frac{\bar{\lambda}(\alpha)}{\alpha(\alpha-1)(\alpha-\bar{s})} \right| \leq \bar{c} \quad \forall \alpha \in (0, \bar{s}) \cup (\bar{s}, 1). \quad (4.12)$$

Let

$$\begin{aligned} X &:= \{\psi \in C^1([0, 1]; \mathbb{R}^N) : \psi(0) = \psi(1) = 0\} \quad \text{and} \\ X_h &:= \left\{ \psi_h = \{\psi_{h,k}\}_{k=0}^M \in (\mathbb{R}^N)^{M+1} : \psi_{h,0} = \psi_{h,M} = 0 \right\} \end{aligned}$$

equipped with the norms  $\|\psi\|_X := \|\psi\|_{C^1([0,1];\mathbb{R}^N)}$  and  $\|\psi_h\|_{X_h} := |\hat{D}_h \psi_h|_\infty + |\psi_h|_\infty$ , respectively. Note that  $X_h$  is the same space as  $Y_h$  but equipped with a different norm. Using (4.11), we obtain by a direct computation that the first variation  $\delta \mathcal{F}(\bar{\varphi}) : X \rightarrow C([0, 1]; \mathbb{R}^N)$  is given by

$$\begin{aligned} \delta \mathcal{F}(\bar{\varphi})\psi(\alpha) &= P_{\bar{\varphi}'(\alpha)}^\perp \left( \nabla^2 E(\bar{\varphi}(\alpha))\psi(\alpha) - \bar{\lambda}(\alpha)\psi'(\alpha) \right) \\ &+ \alpha(\alpha-1)(\alpha-\bar{s}) \left( \frac{\bar{\varphi}'(s)^T \psi'(s)}{|\bar{\varphi}'(s)|} - \int_0^1 \frac{\bar{\varphi}'(s)^T \psi'(s)}{|\bar{\varphi}'(s)|} ds \right) \frac{\bar{\varphi}'(\alpha)}{|\bar{\varphi}'(\alpha)|} \quad \text{for } \alpha \in [0, 1]. \end{aligned} \quad (4.13)$$

For  $\varphi_h \in \mathcal{A}_h$ , we can obtain the first variation  $\delta \mathcal{F}_h(\varphi_h) : X_h \rightarrow Y_h$  by a direct calculation that for  $k = 0, \dots, M$ ,

$$\begin{aligned} (\delta \mathcal{F}_h(\varphi_h)\psi_h)_k &= P_{(\tilde{D}_h \varphi_h)_k}^\perp \left( \nabla^2 E(\varphi_{h,k})\psi_{h,k} - \frac{\nabla E(\varphi_{h,k})^T (\tilde{D}_h \varphi_h)_k}{|(\tilde{D}_h \varphi_h)_k|^2} (\tilde{D}_h \psi_h)_k \right) \\ &- \frac{(P_{(\tilde{D}_h \varphi_h)_k}^\perp \nabla E(\varphi_{h,k}))^T (\tilde{D}_h \psi_h)_k}{|(\tilde{D}_h \varphi_h)_k|} \frac{(\tilde{D}_h \varphi_h)_k}{|(\tilde{D}_h \varphi_h)_k|} \\ &+ \alpha_k(\alpha_k-1)(\alpha_k - \alpha_{k\bar{s}+\frac{1}{2}}) \left( \frac{(\hat{D}_h \psi_h)_k^T (\hat{D}_h \varphi_h)_k}{|(\hat{D}_h \varphi_h)_k|} - h \sum_{t=1}^M \frac{(\hat{D}_h \psi_h)_t^T (\hat{D}_h \varphi_h)_t}{|(\hat{D}_h \varphi_h)_t|} \right) \frac{(\tilde{D}_h \varphi_h)_k}{|(\tilde{D}_h \varphi_h)_k|} \\ &+ \alpha_k(\alpha_k-1)(\alpha_k - \alpha_{k\bar{s}+\frac{1}{2}}) (|(\hat{D}_h \varphi_h)_k| - L_h(\varphi_h)) \frac{P_{(\tilde{D}_h \varphi_h)_k}^\perp (\tilde{D}_h \psi_h)_k}{|(\tilde{D}_h \varphi_h)_k|}. \end{aligned} \quad (4.14)$$

## 4.2 Stability of the discrete MEP

Define a projection operator  $\Pi_h : C([0, 1]; \mathbb{R}^N) \rightarrow (\mathbb{R}^N)^{M+1}$  by

$$(\Pi_h \varphi)_k := \varphi(kh), \quad k = 0, \dots, M.$$

The following lemma states the stability of the discrete MEP, which is a key ingredient in the convergence analysis.

**Lemma 4.2.** *Let  $\bar{\varphi} \in C^3([0, 1]; \mathbb{R}^N)$  be a solution of (2.1). Assume that **(A)** and **(B)** are satisfied. Then for sufficiently small  $h$ , there exists a constant  $C > 0$  depending only on  $E$  and  $\bar{\varphi}$  such that*

$$\|\psi_h\|_{X_h} \leq C \|\delta \mathcal{F}_h(\Pi_h \bar{\varphi})\psi_h\|_{Y_h} \quad \forall \psi_h \in X_h. \quad (4.15)$$

Before proving this lemma, let

$$\hat{X}_h := \left\{ \hat{\psi}_h \in X : \hat{\psi}_h|_{[\alpha_{k-1}, \alpha_k]} \text{ is a cubic polynomial for } 1 \leq k \leq M \right. \\ \left. \text{and } \hat{\psi}_h \text{ satisfying } \hat{\psi}'_h(\alpha_k) = (\tilde{D}_h \Pi_h \hat{\psi}_h)_k \text{ for } 0 \leq k \leq M \right\} \quad (4.16)$$

equipped with the norm  $\|\cdot\|_X$ . We see that  $\dim(\hat{X}_h) = N(M-1)$  and any  $\hat{\psi}_h \in \hat{X}_h$  can be determined by their values at the nodes  $\alpha_k$  ( $1 \leq k \leq M-1$ ). Thus  $\Pi_h : \hat{X}_h \rightarrow X_h$  is an isomorphism. Denote its inverse operator by  $P_h : X_h \rightarrow \hat{X}_h$  satisfying

$$P_h \psi_h(\alpha_k) = \psi_{h,k} \quad \text{for } k = 0, \dots, M. \quad (4.17)$$

Given  $\hat{\psi}_h \in \hat{X}_h$ , let

$$f_h = \Pi_h \delta \mathcal{F}(\bar{\varphi}) \hat{\psi}_h. \quad (4.18)$$

To show Lemma 4.2, we will first bring in a basis set of  $\hat{X}_h$  to derive a spectral representation of (4.18) and obtain some linear systems. Then by analyzing the coefficient matrices we will show that the operator  $\Pi_h \delta \mathcal{F}(\bar{\varphi}) : \hat{X}_h \rightarrow Y_h$  is invertible and  $\left\| (\Pi_h \delta \mathcal{F}(\bar{\varphi}))^{-1} \right\|_{\mathcal{L}(Y_h, \hat{X}_h)}$  is uniformly bounded with respect to  $h$ . Finally, Lemma 4.2 follows from a perturbation argument.

For  $\alpha \in [0, 1]$ , we consider the eigenvalue problem

$$\left( P_{\bar{\varphi}'(\alpha)}^\perp \nabla^2 E(\bar{\varphi}(\alpha)) P_{\bar{\varphi}'(\alpha)}^\perp \right) \xi_i(\alpha) = z_i(\alpha) \xi_i(\alpha) \quad \text{for } i = 0, 1, \dots, N-1 \quad (4.19)$$

with  $\{z_i(\alpha)\}_{i=0}^{N-1}$  the eigenvalues and  $\{\xi_i(\alpha)\}_{i=0}^{N-1}$  the corresponding eigenfunctions. From [11], we can order the functions  $z_i(\alpha)$  such that  $z_0(\bar{s}) \leq z_1(\bar{s}) \leq \dots \leq z_{N-1}(\bar{s})$  and  $z_i \in C^2([0, 1]; \mathbb{R})$ ,  $\xi_i \in C^2([0, 1]; \mathbb{R}^N)$  for  $i = 0, 1, \dots, N-1$ . Moreover, we have  $z_0(\alpha) \equiv 0$ ,  $\xi_0(\alpha) \equiv \bar{\varphi}'(\alpha)/|\bar{\varphi}'(\alpha)|$  and

$$z_j(\alpha) > 0 \quad \text{for } j = 1, \dots, N-1, \alpha = 0, \bar{s}, 1. \quad (4.20)$$

Let  $g_{h,k,j} \in \hat{X}_h$  ( $1 \leq k \leq M-1$ ,  $0 \leq j \leq N-1$ ) be a set of functions satisfying

$$g_{h,k,j}(\alpha_t) = \delta_{kt} \xi_j(\alpha_t) \quad \text{for } t = 1, \dots, M-1. \quad (4.21)$$

Note that  $\{g_{h,k,j}\}$  gives a complete basis set for the finite dimensional space  $\hat{X}_h$ , since any function  $\hat{\psi}_h \in \hat{X}_h$  can be determined by their values at the nodes  $\alpha_k$  ( $1 \leq k \leq M-1$ ).

Now we can represent  $\hat{\psi}_h$  in (4.18) by the basis  $\{g_{h,k,j}\}$  ( $1 \leq k \leq M-1$ ,  $0 \leq j \leq N-1$ )

$$\hat{\psi}_h(\alpha) = \sum_{k=1}^{M-1} \sum_{j=0}^{N-1} \gamma_{k,j} g_{h,k,j}(\alpha) \quad (4.22)$$

with  $\{\gamma_{k,j}\}$  the unknown coefficients. As the operator  $\delta \mathcal{F}(\bar{\varphi})$  (4.13) has completely different behavior in the direction  $\bar{\varphi}'$  and in the subspace  $\bar{\varphi}'^\perp$ , we will project (4.18) into these two subspaces respectively. Define  $\gamma_{M,j} = \gamma_{0,j} = 0$  for  $j = 0, \dots, N-1$ . Denote  $\gamma^\perp \in (\mathbb{R}^{N-1})^{M+1}$  and  $\gamma_0 \in \mathbb{R}^{M+1}$  with

$$\gamma_k^\perp := \{\gamma_{k,j}\}_{j=1}^{N-1}, \quad (\gamma_0)_k := \gamma_{k,0} \quad \text{for } k = 0, \dots, M, \quad (4.23)$$

Denote  $F^\perp \in (\mathbb{R}^{N-1})^{M-1}$  and  $F_0 \in \mathbb{R}^{M-1}$  with

$$F_k^\perp := \{\xi_j(\alpha_k)^T f_{h,k}\}_{j=1}^{N-1}, \quad (F_0)_k := \xi_0(\alpha_k)^T f_{h,k} \quad \text{for } k = 1, \dots, M-1. \quad (4.24)$$

We first consider the problem (4.18) in the subspace perpendicular to the tangent of MEP  $\xi_0 = \bar{\varphi}'/|\bar{\varphi}'|$ . By substituting (4.22) into (4.18), taking  $k$ -th component, multiplying both sides with  $\xi_j(\alpha_k)^T$ ,  $1 \leq j \leq N-1$ , using (4.11), (4.19) and (4.21), we obtain by a direct calculation that

$$A(\alpha_k)\gamma_k^\perp - \bar{\lambda}(\alpha_k)(\tilde{D}_h\gamma^\perp)_k = F_k^\perp \quad \text{for } k = 1, \dots, M-1, \quad (4.25)$$

where

$$A(\alpha) := \text{Diag}(z_1(\alpha), z_2(\alpha), \dots, z_{N-1}(\alpha)) = \begin{pmatrix} z_1(\alpha) & & & \\ & z_2(\alpha) & & \\ & & \ddots & \\ & & & z_{N-1}(\alpha) \end{pmatrix} \quad (4.26)$$

for  $\alpha \in [0, 1]$ . Note that the linear system (4.25) is independent of  $\gamma_0$ .

To better estimate  $\|\hat{\psi}_h\|_X$  by  $\|f_h\|_{Y_h}$ , we transform the linear system (4.25) into another form. We know from (4.3) that  $(\tilde{D}_h\gamma^\perp)_{k_{\bar{s}}} = \frac{1}{2}((\tilde{D}_h\gamma^\perp)_{k_{\bar{s}+1}} + (\tilde{D}_h\gamma^\perp)_{k_{\bar{s}-1}})$ . Taking  $k = k_{\bar{s}} - 1, k_{\bar{s}}, k_{\bar{s}} + 1$  in (4.25), we obtain the following linear system:

$$P_{h,\bar{s}} \begin{pmatrix} (\tilde{D}_h\gamma^\perp)_{k_{\bar{s}-1}} \\ (\tilde{D}_h\gamma^\perp)_{k_{\bar{s}+1}} \\ \gamma_{k_{\bar{s}}}^\perp \end{pmatrix} = \begin{pmatrix} \frac{F_{k_{\bar{s}-1}}^\perp - F_{k_{\bar{s}}}^\perp}{-h} \\ \frac{F_{k_{\bar{s}+1}}^\perp - F_{k_{\bar{s}}}^\perp}{h} \\ F_{k_{\bar{s}}}^\perp \end{pmatrix}, \quad (4.27)$$

where

$$P_{h,\bar{s}} := \begin{pmatrix} B_{k_{\bar{s}-1}} - \frac{\bar{\lambda}(\alpha_{k_{\bar{s}}})}{2h}I & -\frac{\bar{\lambda}(\alpha_{k_{\bar{s}}})}{2h}I & \frac{A(\alpha_{k_{\bar{s}}}) - A(\alpha_{k_{\bar{s}-1}})}{h} \\ -\frac{\bar{\lambda}(\alpha_{k_{\bar{s}}})}{2h}I & B_{k_{\bar{s}+1}} - \frac{\bar{\lambda}(\alpha_{k_{\bar{s}}})}{2h}I & \frac{A(\alpha_{k_{\bar{s}+1}}) - A(\alpha_{k_{\bar{s}}})}{h} \\ -\frac{\bar{\lambda}(\alpha_{k_{\bar{s}}})}{2}I & -\frac{\bar{\lambda}(\alpha_{k_{\bar{s}}})}{2}I & A(\alpha_{k_{\bar{s}}}) \end{pmatrix} \quad \text{with} \quad (4.28)$$

$$B_{k_{\bar{s}-1}} := I + h \frac{A(\alpha_{k_{\bar{s}-1}})}{\bar{\lambda}(\alpha_{k_{\bar{s}-1}})} \quad \text{and} \quad B_{k_{\bar{s}+1}} := I - h \frac{A(\alpha_{k_{\bar{s}+1}})}{\bar{\lambda}(\alpha_{k_{\bar{s}+1}})}.$$

For any  $\delta \in (0, \frac{\bar{s}}{2})$ , there exists a  $k_\delta \in \mathbb{Z}_+$  such that

$$k_\delta h \leq \delta < (k_\delta + 1)h. \quad (4.29)$$

Taking  $k = 1, \dots, k_{\bar{s}} - 2$  in (4.25) and combining with

$$-h \sum_{t=k}^{k_{\bar{s}}-1} (\tilde{D}_h\gamma^\perp)_t + \gamma_{k_{\bar{s}}}^\perp = \gamma_k^\perp = h \sum_{t=0}^{k-1} (\tilde{D}_h\gamma^\perp)_t, \quad h \sum_{t=0}^{k_\delta} (\tilde{D}_h\gamma^\perp)_t = \gamma_{k_\delta+1}^\perp,$$

we obtain the following linear systems:

$$\begin{aligned} \frac{B_k}{\alpha_k - \alpha_{k_{\bar{s}}}} (\tilde{D}_h \gamma^\perp)_k &= \frac{A(\alpha_k) - A(\alpha_{k_{\bar{s}}})}{\alpha_k - \alpha_{k_{\bar{s}}}} \gamma_{k_{\bar{s}}}^\perp + \frac{\bar{\lambda}(\alpha_{k_{\bar{s}}})}{\alpha_k - \alpha_{k_{\bar{s}}}} (\tilde{D}_h \gamma^\perp)_{k_{\bar{s}}} \\ &- \frac{F_k^\perp - F_{k_{\bar{s}}}^\perp}{\alpha_k - \alpha_{k_{\bar{s}}}} - \frac{hA(\alpha_k)}{\alpha_k - \alpha_{k_{\bar{s}}}} \sum_{t=k+1}^{k_{\bar{s}}-1} (\tilde{D}_h \gamma^\perp)_t \quad \text{for } k_{\bar{s}} - k_\delta \leq k \leq k_{\bar{s}} - 2, \end{aligned} \quad (4.30)$$

$$B_k (\tilde{D}_h \gamma^\perp)_k = -hA(\alpha_k) \sum_{t=k+1}^{k_{\bar{s}}-1} (\tilde{D}_h \gamma^\perp)_t + A(\alpha_k) \gamma_{k_{\bar{s}}}^\perp - F_k^\perp \quad (4.31)$$

for  $k_\delta + 1 \leq k \leq k_{\bar{s}} - k_\delta - 1$  and

$$P_{h,\delta} \begin{pmatrix} (\tilde{D}_h \gamma^\perp)_0 \\ (\tilde{D}_h \gamma^\perp)_1 \\ \vdots \\ (\tilde{D}_h \gamma^\perp)_{k_\delta} \end{pmatrix} = \begin{pmatrix} \gamma_{k_\delta+1}^\perp \\ \frac{F_1^\perp}{\alpha_1} \\ \dots \\ \frac{F_{k_\delta}^\perp}{\alpha_{k_\delta}} \end{pmatrix}, \quad (4.32)$$

where

$$B_k := I + h \frac{A(\alpha_k)}{\bar{\lambda}(\alpha_k)} \quad \text{for } 1 \leq k \leq k_{\bar{s}} - 2 \quad \text{and} \quad (4.33)$$

$$P_{h,\delta} := \begin{pmatrix} hI & hI & hI & \dots & hI \\ \frac{hA(\alpha_1)}{\alpha_1} & -\frac{\bar{\lambda}(\alpha_1)}{\alpha_1} I & & & \\ \frac{hA(\alpha_2)}{\alpha_2} & \frac{hA(\alpha_2)}{\alpha_2} & -\frac{\bar{\lambda}(\alpha_2)}{\alpha_2} I & & \\ \vdots & \vdots & \vdots & \ddots & \\ \frac{hA(\alpha_{k_\delta})}{\alpha_{k_\delta}} & \frac{hA(\alpha_{k_\delta})}{\alpha_{k_\delta}} & \frac{hA(\alpha_{k_\delta})}{\alpha_{k_\delta}} & \dots & -\frac{\bar{\lambda}(\alpha_{k_\delta})}{\alpha_{k_\delta}} I \end{pmatrix}. \quad (4.34)$$

Note that we have rewritten (4.25) into (4.27), (4.30), (4.31) and (4.32), which are used to bound  $(\tilde{D}_h \gamma^\perp)_k$  at the saddle, near the saddle, between the saddle and the minimizer  $y_M^A$ , and near the minimizer  $y_M^A$ , respectively. Note that for  $k > k_{\bar{s}} + 1$  we have the similar linear systems. To estimate  $|\tilde{D}_h \gamma^\perp|_\infty$ , we only need to analyze the coefficient matrix in these linear systems.

We then consider the problem in the tangent direction  $\tilde{\varphi}'$ . By substituting (4.22) into (4.18), taking  $k$ -th component, multiplying both sides with  $\xi_0(\alpha_k)^T$ , we obtain

$$\alpha_k(\alpha_k - 1)(\alpha_k - \bar{s}) \left( (\tilde{D}_h \gamma_0)_k - \sum_{i=0}^{N-1} \sum_{t=1}^{M-1} \gamma_{t,i} c_{h,t,i} \right) = (F_0)_k \quad \text{for } k = 1, \dots, M-1, \quad (4.35)$$

where

$$c_{h,t,i} := \int_0^1 g_{h,t,i}(s)^T \xi_0'(s) ds \quad \text{for } \alpha \in [0, 1]. \quad (4.36)$$

We see that  $\gamma_0$  depends on the component  $\gamma^\perp$ . In our analysis, we will first focus on the problem (4.25) in the subspace  $\bar{\varphi}^\perp$ , and then put things back into (4.35) in tangent direction  $\bar{\varphi}'$ .

So far, we have obtained a spectral representation of (4.18). Now we define a suitable  $\delta$  and turn to the analysis of the coefficient matrices in (4.27), (4.30), (4.31) and (4.32). Define

$$\sigma_j := \frac{z_j(0)}{\bar{\lambda}'(0)} \quad \text{for } 1 \leq j \leq N-1 \quad \text{and} \quad (4.37)$$

$$n_j(\alpha) := \frac{z_j(\alpha)}{\bar{\lambda}(\alpha)} - \frac{\sigma_j}{\alpha} \quad \text{for } \alpha \in (0, \frac{\bar{s}}{2}], 1 \leq j \leq N-1 \quad (4.38)$$

We have from assumption **(B)** that  $\sigma_j > 1$  for  $1 \leq j \leq N-1$ . Since

$$\begin{aligned} \left| \lim_{\alpha \rightarrow 0^+} n_j(\alpha) \right| &= \left| \lim_{\alpha \rightarrow 1^-} \frac{z_j(\alpha)\alpha - \sigma_j \bar{\lambda}(\alpha)}{\alpha \bar{\lambda}(\alpha)} \right| = \left| \lim_{\alpha \rightarrow 1^-} \frac{z_j'(\alpha)\alpha + z_j(\alpha) - \sigma_j \bar{\lambda}'(\alpha)}{\alpha \bar{\lambda}'(\alpha) + \bar{\lambda}(\alpha)} \right| \\ &= \left| \lim_{\alpha \rightarrow 0^+} \frac{2z_j'(\alpha) + z_j''(\alpha)\alpha - \sigma_j \bar{\lambda}''(\alpha)}{\alpha \bar{\lambda}''(\alpha) + 2\bar{\lambda}'(\alpha)} \right| = \left| \frac{2z_j'(0) - \sigma_j \bar{\lambda}''(0)}{2\bar{\lambda}'(0)} \right| < C \end{aligned} \quad (4.39)$$

with  $C$  a constant depending only on  $\bar{\lambda}$  and  $z_j$ , we have that  $n_j$  is bounded on  $(0, \frac{\bar{s}}{2}]$ . Define

$$\bar{\sigma} := \frac{1}{2} \left( 1 + \max_{1 \leq j \leq N-1} \sigma_j \right). \quad (4.40)$$

From the fact that  $\sigma_j > 1$  for  $1 \leq j \leq N-1$ , we have  $\bar{\sigma} > 1$ . Therefore, there exists  $\delta \in (0, \frac{\bar{s}}{2})$  such that  $z_j(\alpha) > 0$  for  $\alpha \in [\bar{s} - \delta - 2h, \bar{s} + h]$ ,  $1 \leq j \leq N-1$ ,  $\frac{1}{2}\bar{\lambda}'(0) \leq \|\bar{\lambda}'\|_{C([0, \delta]; \mathbb{R})} \leq 2\bar{\lambda}'(0)$  and

$$\frac{\sigma_j - \bar{\sigma}}{\delta} \geq \|n_j\|_{C((0, \frac{\bar{s}}{2}]; \mathbb{R})} \quad \text{for } 1 \leq j \leq N-1. \quad (4.41)$$

This together with (4.38) implies

$$\frac{z_j(\alpha)}{\bar{\lambda}(\alpha)} = \frac{\sigma_j}{\alpha} + n_j(\alpha) \geq \frac{\bar{\sigma}}{\alpha} \quad \forall \alpha \in (0, \delta]. \quad (4.42)$$

**Lemma 4.3.** *Under the assumption of Lemma 4.2, let  $\bar{\sigma}$ ,  $\delta$ ,  $k_\delta$  and  $B_k$ ' be given by (4.40), (4.41), (4.29) and (4.33), respectively. Then for sufficient small  $h$ ,  $B_k$ 's are invertible and there exist a constant  $C > 0$  depending only on  $\bar{\lambda}$  and  $A$  such that*

$$\|B_k^{-1}\|_\infty \leq \frac{\bar{\sigma}}{k + \bar{\sigma}} \quad \text{for } 1 \leq k \leq k_\delta, \quad (4.43)$$

$$\|B_k^{-1}\|_\infty \leq 1 + Ch \quad \text{for } k_\delta + 1 \leq k \leq k_{\bar{s}} - k_\delta - 1, \quad (4.44)$$

$$\|B_k^{-1}\|_\infty < \frac{1}{\alpha_{k_{\bar{s}}} - \alpha_k} \quad \text{for } k_{\bar{s}} - k_\delta \leq k \leq k_{\bar{s}} - 2, \quad (4.45)$$

where the constants  $C$  depend only on  $\bar{\lambda}$  and  $A$ . Moreover, we have

$$\|B_k^{-1} - I\|_\infty \leq \frac{C}{k} \quad \text{for } 1 \leq k \leq k_\delta. \quad (4.46)$$



*Proof.* Since  $B_k$  is a diagonal matrix, we have

$$\|B_k^{-1}\|_\infty = \max_{1 \leq j \leq N-1} \left| \frac{1}{1 + \frac{z_j(\alpha_k)h}{\lambda(\alpha_k)}} \right| \quad \text{and} \quad \|B_k^{-1} - I\|_\infty = \max_{1 \leq j \leq N-1} \left| \frac{\frac{z_j(\alpha_k)h}{\lambda(\alpha_k)}}{1 + \frac{z_j(\alpha_k)h}{\lambda(\alpha_k)}} \right| \quad (4.47)$$

for  $1 \leq k \leq k_{\bar{s}} - 1$ . For  $1 \leq k \leq k_\delta$ , using (4.40) and (4.42) yields

$$1 + \frac{z_j(\alpha_k)h}{\lambda(\alpha_k)} \geq 1 + \frac{\bar{\sigma}h}{\alpha_k} \geq 1 + \frac{\bar{\sigma}}{k} \quad \text{for } 1 \leq j \leq N-1.$$

This together with (4.47) leads to

$$\|B_k^{-1}\|_\infty \leq \frac{k}{k + \bar{\sigma}} \quad \text{and} \quad \|B_k^{-1} - I\|_\infty \leq \frac{Ch}{\lambda(\alpha_k)} \leq \frac{C}{k} \frac{\alpha_k}{\int_0^{\alpha_k} |\bar{\lambda}'(s)| ds} \leq \frac{C}{k},$$

where  $C$  depends on  $\bar{\lambda}$  and  $A$ . This completes the proof for (4.43) and (4.46).

For  $k_\delta + 1 \leq k \leq k_{\bar{s}} - k_\delta - 1$ , since  $|\bar{\lambda}(\alpha_k)|$  have both upper bound and lower bound, we have from (4.47) that

$$\|B_k^{-1}\|_\infty \leq \frac{1}{1 - Ch} \leq 1 + Ch,$$

where  $C$  depends on  $\bar{\lambda}$  and  $A$ . This completes the proof for (4.44).

For  $k_{\bar{s}} - k_\delta \leq k \leq k_{\bar{s}} - 2$ , using the fact that  $z_j(\alpha_k) > 0$  and  $\bar{\lambda}(\alpha_k) > 0$ , we obtain

$$\|B_k^{-1}\|_\infty = \max_{1 \leq j \leq N-1} \frac{1}{1 + \frac{z_j(\alpha_k)h}{\lambda(\alpha_k)}} < 1 < \frac{1}{\alpha_{k_{\bar{s}}} - \alpha_k}. \quad \square$$

**Lemma 4.4.** *Under the assumption of Lemma 4.2, let  $\delta$ ,  $k_\delta$ ,  $P_{h,\bar{s}}$  and  $P_{h,\delta}$  be given by (4.41), (4.29), (4.28) and (4.34), respectively. Then for sufficiently small  $h$ ,  $P_{h,\bar{s}}$  and  $P_{h,\delta}$  are invertible and there exist constants  $C > 0$  depending on  $\bar{\lambda}$  and  $A$  such that*

$$\|P_{h,\bar{s}}^{-1}\|_\infty \leq C \quad \text{and} \quad \|P_{h,\delta}^{-1}\|_\infty \leq C. \quad (4.48)$$

*Proof.* Since  $\lim_{h \rightarrow 0^+} \alpha_{k_{\bar{s}}} = \bar{s}$  and  $\bar{\lambda}(\bar{s}) = 0$ , we have

$$P_{\bar{s}} := \lim_{h \rightarrow 0^+} P_{h,\bar{s}} = \begin{pmatrix} B_{\bar{s}} & A'(\bar{s}) \\ & B_{\bar{s}} & A'(\bar{s}) \\ & & & A(\bar{s}) \end{pmatrix}, \quad P_{\bar{s}}^{-1} = \begin{pmatrix} B_{\bar{s}}^{-1} & & & -B_{\bar{s}}^{-1} A'(\bar{s}) A(\bar{s})^{-1} \\ & B_{\bar{s}}^{-1} & & -B_{\bar{s}}^{-1} A'(\bar{s}) A(\bar{s})^{-1} \\ & & & \\ & & & A(\bar{s})^{-1} \end{pmatrix},$$

where  $B_{\bar{s}} := I - \frac{A(\bar{s})}{\bar{\lambda}'(\bar{s})} \in \mathbb{R}^{(N-1) \times (N-1)}$ . From Lemma 4.1 (ii) and the fact that  $z_j(\bar{s}) > 0$  for  $1 \leq j \leq N-1$ , we obtain

$$\|B_{\bar{s}}^{-1}\|_\infty \leq \max_{1 \leq j \leq N-1} \frac{1}{1 - \frac{z_j(\bar{s})}{\bar{\lambda}'(\bar{s})}} \leq 1, \quad \|A(\bar{s})^{-1}\|_\infty \leq \max_{1 \leq j \leq N-1} \frac{1}{z_j(\bar{s})}.$$

This implies

$$\|P_{\bar{s}}^{-1}\|_\infty \leq \|B_{\bar{s}}^{-1}\|_\infty + \|B_{\bar{s}}^{-1}\|_\infty \|A'(\bar{s})\|_\infty \|A(\bar{s})^{-1}\|_\infty + \|A(\bar{s})^{-1}\|_\infty \leq C,$$

where  $C$  depends only on  $\bar{\lambda}$  and  $A$ . Thus  $P_{h,\bar{s}}$  is invertible and  $\|P_{h,\bar{s}}\|_\infty \leq C$  for sufficiently small  $h$ . This completes the proof for first part of (4.48).

We then investigate the inverse of  $P_{h,\delta}$ :

$$P_{h,\delta}^{-1} = Q_{h,\delta} T_{h,\delta}, \quad (4.49)$$

where

$$Q_{h,\delta} := \begin{pmatrix} h^{-1}B_1^{-1} \cdots B_{k_\delta}^{-1} & -B_1^{-1} & -B_1^{-1}B_2^{-1} & \cdots & -B_1^{-1} \cdots B_{k_\delta}^{-1} \\ h^{-1}(I - B_1^{-1})B_2^{-1} \cdots B_{k_\delta}^{-1} & B_1^{-1} & (B_1^{-1} - I)B_2^{-1} & \cdots & (B_1^{-1} - I)B_2^{-1} \cdots B_{k_\delta}^{-1} \\ h^{-1}(I - B_2^{-1})B_3^{-1} \cdots B_{k_\delta}^{-1} & & B_2^{-1} & \cdots & (B_2^{-1} - I)B_3^{-1} \cdots B_{k_\delta}^{-1} \\ \vdots & & & \ddots & \\ h^{-1}(I - B_{k_\delta}^{-1}) & & & & B_{k_\delta}^{-1} \end{pmatrix},$$

$$T_{h,\delta} := \begin{pmatrix} I & & & & \\ & -\frac{\alpha_1}{\lambda(\alpha_1)}I & & & \\ & & \ddots & & \\ & & & & -\frac{\alpha_{k_\delta}}{\lambda(\alpha_{k_\delta})}I \end{pmatrix}.$$

We see from Lemma 4.1 (iii) that  $\|T_{h,\delta}\|_\infty \leq C$  where  $C$  only depends on  $\bar{\lambda}$  and  $\delta$ . To estimate  $\|Q_{h,\delta}\|_\infty$ , we first present two inequalities. We claim that there exist constants  $C_1, C_2, C > 0$  depending only on  $\bar{\sigma}$  such that

$$C_1 \frac{1}{n^{\bar{\sigma}}} \leq \prod_{s=1}^n \frac{s}{s + \bar{\sigma}} \leq C_2 \frac{1}{n^{\bar{\sigma}}} \quad \text{for } n \in \mathbb{Z}_+ \quad \text{and} \quad (4.50)$$

$$\frac{1}{n^{\bar{\sigma}}} \leq C \left( \frac{1}{(n-1)^{\bar{\sigma}-1}} - \frac{1}{n^{\bar{\sigma}-1}} \right) \quad \text{for } n \geq 2, \quad (4.51)$$

The inequality (4.50) results from induction and the fact that

$$\lim_{n \rightarrow +\infty} \frac{n+1}{n+1+\bar{\sigma}} = 1 = \lim_{n \rightarrow +\infty} \frac{n^{\bar{\sigma}}}{(n+1)^{\bar{\sigma}}}.$$

Using the monotonicity, there exists a constant  $C > 0$  depending on  $\bar{\sigma}$  such that

$$\frac{1}{n} \leq \frac{1}{2} \leq C(2^{\bar{\sigma}-1} - 1) \leq C \left( \frac{n^{\bar{\sigma}-1}}{(n-1)^{\bar{\sigma}-1}} - 1 \right) \quad \forall n \geq 2,$$

which leads to (4.51) by multiplying  $n^{1-\bar{\sigma}}$  on both sides.

Applying (4.50) and Lemma 4.3, we first estimate

$$\left\| \prod_{t=k+1}^{k'} B_t^{-1} \right\|_\infty \leq \prod_{t=k+1}^{k'} \frac{t}{t + \bar{\sigma}} \leq C \frac{(k+1)^{\bar{\sigma}}}{(k')^{\bar{\sigma}}} \leq C(k+1)^{\bar{\sigma}} \left( \frac{1}{(k'-1)^{\bar{\sigma}-1}} - \frac{1}{(k')^{\bar{\sigma}-1}} \right) \quad (4.52)$$

for  $1 \leq k < k' \leq k_\delta$ . Since  $k_\delta$  scales as  $O(h^{-1})$ , using (4.52) and Lemma 4.3, we obtain

$$\|h^{-1}B_1^{-1} \cdots B_{k_\delta}^{-1}\|_\infty \leq \frac{C}{h(k_\delta)^{\bar{\sigma}}} \leq C, \quad (4.53)$$

$$\sum_{k=2}^{k_\delta} \left\| \prod_{t=1}^k B_t^{-1} \right\|_\infty \leq C \sum_{k=2}^{k_\delta} \left( \frac{1}{(k-1)^{\bar{\sigma}-1}} - \frac{1}{k^{\bar{\sigma}-1}} \right) \leq C \left( 1 - \frac{1}{k_\delta^{\bar{\sigma}-1}} \right) \leq C, \quad (4.54)$$

and

$$\begin{aligned} \sum_{t=k+1}^{k_\delta} \|(B_k^{-1} - I) \prod_{t'=k+1}^t B_{t'}^{-1}\|_\infty &\leq \frac{C(k+1)^{\bar{\sigma}}}{k} \sum_{t=k+1}^{k_\delta} \left( \frac{1}{(t-1)^{\bar{\sigma}-1}} - \frac{1}{t^{\bar{\sigma}-1}} \right) \\ &\leq \frac{C(k+1)}{k} \left( \frac{(k+1)^{\bar{\sigma}-1}}{k^{\bar{\sigma}-1}} - \frac{(k+1)^{\bar{\sigma}-1}}{k_\delta^{\bar{\sigma}-1}} \right) \leq C, \end{aligned} \quad (4.55)$$

$$\|h^{-1}(I - B_k^{-1}) \prod_{t=k+1}^{k_\delta} B_t^{-1}\|_\infty \leq \frac{C}{kh} \frac{(k+1)^{\bar{\sigma}}}{(k_\delta)^{\bar{\sigma}}} \leq C \quad (4.56)$$

for  $1 \leq k \leq k_\delta - 1$ . Combining (4.53)-(4.56), we have from (4.49) that

$$\|P_{h,\delta}^{-1}\|_\infty \leq \|Q_{h,\delta}\|_\infty \|T_{h,\delta}\|_\infty \leq C,$$

where  $C$  only depends on  $\bar{\lambda}$ ,  $\delta$  and  $\bar{\sigma}$ . This completes the proof of (4.48).  $\square$

Before proving Lemma 4.2, we give the discretization error of the operators  $\tilde{D}_h$ ,  $\hat{D}_h$  and  $L_h$ . Given  $\varphi \in C^2([0, 1]; \mathbb{R}^N) \cap \mathcal{A}$ , we see from (4.3) and (4.4) that there exists a constant  $C > 0$  independent of  $h$ , such that

$$|\tilde{D}_h \Pi_h \varphi - \Pi_h \varphi'|_\infty + |\hat{D}_h \Pi_h \varphi - \Pi_h \varphi'|_\infty \leq Ch. \quad (4.57)$$

This together with the standard error estimate of the numerical integration leads to

$$|L_h(\Pi_h \varphi) - L(\varphi)| \leq \left| h \sum_{t=1}^M (|\hat{D}_h \Pi_h \varphi|_t - |\varphi'(\alpha_t)|) \right| + \left| h \sum_{t=1}^M \varphi'(\alpha_t) - \int_0^1 |\varphi'(s)| ds \right| \leq Ch. \quad (4.58)$$

We obtain by a similar argument that

$$|\delta L_h(\Pi_h \varphi) \psi_h - \delta L(\varphi)(P_h \psi_h)| \leq Ch \quad \forall \psi_h \in X_h, \quad (4.59)$$

where  $P_h$  is defined in (4.17).

Now we are ready to show the stability of the discrete MEP.

*Proof of Lemma 4.2.* For any  $\psi_h \in X_h$ , we have

$$\delta \mathcal{F}_h(\Pi_h \bar{\varphi}) \psi_h = (\delta \mathcal{F}_h(\Pi_h \bar{\varphi}) \psi_h - \Pi_h \delta \mathcal{F}(\bar{\varphi})(P_h \psi_h)) + \Pi_h \delta \mathcal{F}(\bar{\varphi})(P_h \psi_h). \quad (4.60)$$

By comparing  $\delta \mathcal{F}_h(\Pi_h \bar{\varphi}) \psi_h$  in (4.14) and  $\delta \mathcal{F}(\bar{\varphi})(P_h \psi_h)$  in (4.13), using (4.57), (4.58) and (4.59), we obtain

$$\|\delta \mathcal{F}_h(\Pi_h \bar{\varphi}) \psi_h - \Pi_h \delta \mathcal{F}(\bar{\varphi})(P_h \psi_h)\|_{Y_h} \leq Ch \|P_h \psi_h\|_X \leq Ch \|\psi_h\|_{X_h}, \quad (4.61)$$

where  $C$  depends only on  $E$  and  $\bar{\varphi}$ .

Now we turn to the second term in (4.60). For any  $\psi_h \in X_h$ , let  $\hat{\psi}_h = P_h \psi_h$  and  $f_h = \Pi_h \delta \mathcal{F}(\bar{\varphi}) \hat{\psi}_h$ . With the representation (4.22), using Lemma 4.3 and Lemma 4.4, we have from (4.27), (4.30), (4.31) and (4.32) that

$$|(\tilde{D}_h \gamma^\perp)_k|_\infty \leq C \|F^\perp\|_{Y_h} \quad \text{for } 0 \leq k \leq k_{\bar{s}} + 1,$$

where  $\gamma^\perp$  and  $F^\perp$  are given by (4.23) and (4.24), respectively. A similar estimate holds for  $k_{\bar{s}} + 2 \leq k \leq M$  and then we have

$$|\tilde{D}_h \gamma^\perp|_\infty \leq C \|F^\perp\|_{Y_h} \leq C \|f_h\|_{Y_h}, \quad (4.62)$$

where  $C$  depends only on  $\bar{\lambda}$  and  $A$ . We obtain by taking  $k = 1, \dots, k_{\bar{s}} - 1, k_{\bar{s}} + 1, \dots, M - 1$  in (4.35) that

$$|\tilde{D}_h \gamma_0|_\infty \leq \|F_0\|_{Y_h} + |\gamma^\perp|_\infty \sum_{t=1}^{M-1} \sum_{j=1}^{N-1} |c_{h,t,j}| + |\gamma_0|_\infty \sum_{t=1}^{M-1} |c_{h,t,0}|, \quad (4.63)$$

where  $\gamma_0$ ,  $F_0$  and  $c_{h,t,i}$  are given by (4.23), (4.24) and (4.36), respectively. From the definition of  $g_{h,t,i}$  in (4.21) and  $\hat{X}_h$  in (4.16), we know that  $\text{supp}(g_{h,t,i}) \subset [\alpha_{t-2}, \alpha_{t+2}]$  for  $1 \leq t \leq M - 1$ ,  $0 \leq i \leq N - 1$ . Since  $\xi_0 \in C^2([0, 1]; \mathbb{R}^N)$  and  $|\xi_0(\alpha)|^2 \equiv 1$ , we have

$$|c_{h,t,0}| \leq 4h \|\xi_0(\alpha_t)^T \xi_0'(\alpha)\|_{C([\alpha_{t-2}, \alpha_{t+2}]; \mathbb{R})} \leq Ch^2 \quad \text{and} \quad (4.64)$$

$$|c_{h,t,j}| \leq 4h \|g_{h,t,j}^T \xi_0'\|_{C([\alpha_{t-2}, \alpha_{t+2}]; \mathbb{R})} \leq Ch, \quad (4.65)$$

where  $C$  depends only on  $\{\xi_i\}_{i=0}^{N-1}$ . Combining (4.62)-(4.65), we have for sufficiently small  $h$  that

$$|\tilde{D}_h \gamma_0|_\infty \leq C |\gamma^\perp|_\infty + C \|F_0\|_{Y_h} \leq C \|f_h\|_{Y_h}. \quad (4.66)$$

From (4.22) we have

$$\begin{aligned} (\hat{D}_h \psi_h)_k &= h^{-1} \sum_{i=0}^{N-1} (\gamma_{k,i} \xi_i(\alpha_k) - \gamma_{k-1,i} \xi_i(\alpha_{k-1})) \\ &= \sum_{i=0}^{N-1} \left( \frac{\gamma_{k,i} - \gamma_{k-1,i}}{h} \xi_i(\alpha_k) + \gamma_{k-1,i} \frac{\xi_i(\alpha_k) - \xi_i(\alpha_{k-1})}{h} \right) \quad \text{for } 1 \leq k \leq M. \end{aligned}$$

This together with (4.62) and (4.66) implies that for sufficient small  $h$ , there exists a  $C > 0$  depending only on  $\bar{\lambda}$ ,  $A$  and  $\{\xi_i\}_{i=0}^{N-1}$  such that

$$\|\psi_h\|_{X_h} \leq C \left| \begin{pmatrix} \tilde{D}_h \gamma^\perp \\ \tilde{D}_h \gamma_0 \end{pmatrix} \right|_\infty \leq C \|f_h\|_{Y_h}.$$

This indicates

$$\|\psi_h\|_{X_h} \leq C \|\Pi_h \delta_{\mathcal{F}}(\bar{\varphi})(P_h \psi_h)\|_{Y_h} \quad \forall \psi_h \in X_h. \quad (4.67)$$

Combining (4.60), (4.61) and (4.67) yields our stated result.  $\square$

### 4.3 Convergence analysis

Now we are ready to prove the convergence and convergence rate of the approximation  $\bar{\varphi}_h$  with respect to the mesh size  $h$ .

**Theorem 4.1.** *Let  $\bar{\varphi} \in C^3([0, 1]; \mathbb{R}^N)$  be a solution of (2.1). Assume that **(A)** and **(B)** are satisfied. Then for sufficiently small  $h$ , there exist a solution  $\bar{\varphi}_h \in \mathcal{A}_h$  of (4.8) and a constant  $C$  depending only on  $\bar{\varphi}$  and  $E$ , such that*

$$\|\bar{\varphi}_h - \Pi_h \bar{\varphi}\|_{X_h} \leq Ch.$$

*Proof.* The proof is divided into three parts. We will first show the consistency and stability of the discrete MEP equation (4.8), and then derive the convergence by inverse function theorem.

1. *Consistency.* By comparing (4.6) and (4.1), we have from (4.57) and (4.58) that

$$\|\mathcal{F}_h(\Pi_h\bar{\varphi})\|_{Y_h} = \|\mathcal{F}_h(\Pi_h\bar{\varphi}) - \Pi_h\mathcal{F}(\bar{\varphi})\|_{Y_h} \leq Ch, \quad (4.68)$$

where  $C$  only depends on  $E$  and  $\bar{\varphi}$ .

2. *Stability.* It follows directly from Lemma 4.2 that there exists a constant  $C$  depending on  $E$  and  $\bar{\varphi}$  such that

$$\|\delta\mathcal{F}_h(\Pi_h\bar{\varphi})\psi_h\|_{Y_h} \geq C\|\psi_h\|_{X_h} \quad \forall \psi_h \in X_h. \quad (4.69)$$

3. *Application of the inverse function theory.* With the consistency (4.68) and stability (4.69), we can apply the inverse function theorem [13, Lemma 2.2] to obtain that, for  $h$  sufficiently small, the solution  $\bar{\varphi}_h$  of (4.8) exists and

$$\|\bar{\varphi}_h - \Pi_h\bar{\varphi}\|_{X_h} \leq Ch. \quad \square$$

Finally, we can prove Theorem 2.1 by building a connection between the equations (2.5) and (4.8).

*Proof of Theorem 2.1.* Let  $\bar{\varphi}_h$  be a solution of (4.8). Note that the saddle  $y_S$  reaches the energy maximum along the MEP. Then we have from the convergence result in Theorem 4.1 that for sufficiently small  $h$ ,

$$E(\bar{\varphi}_{h,0}) < E(\bar{\varphi}_{h,1}) < \cdots < E(\bar{\varphi}_{h,k_{\bar{s}}}) > E(\bar{\varphi}_{h,k_{\bar{s}}+1}) > \cdots > E(\bar{\varphi}_{h,M}).$$

By comparing (2.4) and (4.3), we see that these two first order difference schemes of  $\bar{\varphi}_h$  are exactly the same, i.e.,  $\tilde{D}_h\bar{\varphi}_h = D_h\bar{\varphi}_h$ . This together with (4.9) yields that  $\bar{\varphi}_h$  is a solution of (2.5) and it remains to show the estimates (2.6) and (2.7).

From (4.57) and Theorem 4.1, we estimate

$$\begin{aligned} \max_{0 \leq k \leq M} \left( |(D_h\bar{\varphi}_h)_k - \bar{\varphi}'(\alpha_k)| + |\bar{\varphi}_{h,k} - \bar{\varphi}(\alpha)| \right) &\leq C(|\tilde{D}_h\bar{\varphi}_h - \Pi_h\bar{\varphi}'|_\infty + |\bar{\varphi}_h - \Pi_h\bar{\varphi}|_\infty) \\ &\leq C|\tilde{D}_h(\bar{\varphi}_h - \Pi_h\bar{\varphi})|_\infty + C|\tilde{D}_h\Pi_h\bar{\varphi} - \Pi_h\bar{\varphi}'|_\infty + C|\bar{\varphi}_h - \Pi_h\bar{\varphi}|_\infty \\ &\leq C|\hat{D}_h(\bar{\varphi}_h - \Pi_h\bar{\varphi})|_\infty + Ch + C|\bar{\varphi}_h - \Pi_h\bar{\varphi}|_\infty \leq Ch, \end{aligned}$$

which completes the proof of (2.6). Then we turn to the error estimate for the energy barrier. Using the fact that  $\nabla E(\bar{\varphi}(\bar{s})) = 0$  and  $E \in C^4(\mathbb{R}^N)$ , we have

$$|\delta E(\bar{\varphi}) - \delta E(\bar{\varphi}_h)| = |E(\bar{\varphi}(\bar{s})) - E(\bar{\varphi}_{h,k_{\bar{s}}})| \leq C|\bar{\varphi}(\bar{s}) - \bar{\varphi}_{h,k_{\bar{s}}}|_\infty^2, \quad (4.70)$$

where  $C$  is a constant depending only on  $E$  and  $\bar{\varphi}$ . Theorem 4.1 and the fact that  $\bar{\varphi} \in C^3([0, 1]; \mathbb{R}^N)$  implies

$$|\bar{\varphi}(\bar{s}) - \bar{\varphi}_{h,k_{\bar{s}}}|_\infty \leq |\bar{\varphi}(\bar{s}) - \bar{\varphi}(\alpha_{k_{\bar{s}}})|_\infty + |\bar{\varphi}(\alpha_{k_{\bar{s}}}) - \bar{\varphi}_{h,k_{\bar{s}}}|_\infty \leq Ch,$$

which together with (4.70) yields (2.7) and completes the proof.  $\square$

## References

- [1] N. Berglund. Kramers' law: Validity, derivations and generalisations. *Markov Process. Related Fields*, 19:459–490, 2013.
- [2] J. Braun and C. Ortner. Sharp uniform convergence rate of the supercell approximation of a crystalline defect. *SIAM J. Numer. Anal.*, 58:279–297, 2020.
- [3] M. Cameron, R. Kohn, and E. Vanden-Eijnden. The string method as a dynamical system. *J. Nonlinear Sci.*, 21:193–230, 2011.
- [4] W. E, W. Ren, and E. Vanden-Eijnden. String method for the study of rare events. *Phys. Rev. B*, 66:052301, 2002.
- [5] W. E, W. Ren, and E. Vanden-Eijnden. Simplified and improved string method for computing the minimum energy paths in barrier-crossing events. *J. Chem. Phys.*, 126:164103, 2007.
- [6] P. Hänggi, P. Talkner, and M. Borkovec. Reaction-rate theory: fifty years after kramers. *Rev. Modern Phys.*, 62:251–341, 1990.
- [7] G. Henkelman, B. P. Uberuaga, and H. Jónsson. A climbing image nudged elastic band method for finding saddle points and minimum energy paths. *J. Chem. Phys.*, 113:9901–9904, 2000.
- [8] H. Jónsson, G. Mills, and K. W. Jacobsen. Nudged elastic band method for finding minimum energy paths of transitions. In *Classical and Quantum Dynamics in Condensed Phase Simulations*, pages 385–404. Citeseer, 1998.
- [9] B. Koten and M. Luskin. Stability and convergence of the string method for computing minimum energy paths. *Multiscale Model. Simul.*, 17:873–898, 2018.
- [10] G. D. Leines and J. Rogal. Comparison of minimum-action and steepest-descent paths in gradient systems. *Phys. Rev. E*, 93:022307, 2016.
- [11] X. Liu, H. Chen, and C. Ortner. Stability of the minimum energy path. *ArXiv e-prints*, 2204.00984, 2022.
- [12] K. Müller and L. D. Brown. Location of saddle points and minimum energy paths by a constrained simplex optimization procedure. *Theor. Chim. Acta*, 53:75–93, 1979.
- [13] C. Ortner. A priori and a posteriori analysis of the quasinonlocal quasicontinuum method in 1d. *Math. Comp.*, 80:1265–1285, 2011.
- [14] C. Ortner, J. Kermode, et al. JuLIP: Julia Library for Interatomic Potentials. <https://github.com/JuliaMolSim/JuLIP.jl>.
- [15] W. Ren and E. Vanden-Eijnden. A climbing string method for saddle point search. *J. Chem. Phys.*, 138:134105, 2013.
- [16] G. H. Vineyard. Frequency factors and isotope effects in solid state rate processes. *J. Phys. Chem. Solids*, 3:121–127, 1957.